Astronomical Techniques and Instruments, Vol. 1, January 2024, 52–61

Article Open Access

Design and analysis of an advanced thermal management system for the solar close observations and proximity experiments spacecraft

Liu Liu[1], Kangli Bao[1], Jianchao Feng[1], Xiaofei Zhu[1], Haoyu Wang[1], Xiaofeng Zhang[1*], Jun Lin[2]

[1]*Innovation Academy for Microsatellites of Chinese Academy of Sciences*, *Shanghai* 201304, *China*

[2]*Yunnan Observatories*, *Chinese Academy of Sciences*, *Kunming* 650216, *China*

*Correspondence: zhangxf@microsate.com

Received: November 20, 2023; Accepted: December 7, 2023; Published Online: December 20, 2023; https://doi.org/10.61977/ati2024007

Citation: Liu, L., Bao, K. L., Feng, J. C., et al. 2024. Design and analysis of an advanced thermal management system for the solar close observations and proximity experiments spacecraft. *Astronomical Techniques and Instruments*, **1**(1): 52−61. https://doi.org/10.61977/ati2024007.

Abstract: In this paper, the mission and the thermal environment of the Solar Close Observations and Proximity Experiments (SCOPE) spacecraft are analyzed, and an advanced thermal management system (ATMS) is designed for it. The relationship and functions of the integrated database, the intelligent thermal control system and the efficient liquid cooling system in the ATMS are elaborated upon. For the complex thermal field regulation system and extreme space thermal environment, a modular simulation and thermal field planning method are proposed, and the feasibility of the planning algorithm is verified by numerical simulation. A solar array liquid cooling system is developed, and the system simulation results indicate that the temperatures of the solar arrays meet the requirements as the spacecraft flies by perihelion and aphelion. The advanced thermal management study supports the development of the SCOPE program and provides a reference for the thermal management in other deep-space exploration programs.

Keywords: Solar Close Observations and Proximity Experiments; Adaptive thermal control method; Thermal field planning method; Pumped liquid cooling system; Advanced thermal management system

1. INTRODUCTION

1.1. Program Background

The Sun, the nearest star to Earth, has been attracting the attention of nations as humanity's pursuit of space exploration continues. In contrast to the extremely distant, dark, and cold environment at the edge of the Solar System, solar exploration is characterized by the brightness and heat in extremely close proximity to the Sun. In the last 15 years, many spacecrafts have been launched for solar exploration, including the Solar Dynamics Observatory (SDO)[1,2], the Parker Solar Probe (PSP)[3], the Solar Orbiter[4], the Advanced Space-based Solar Observatory (ASO-S)[5-7] and the Chinese Hα Solar Explorer (CHASE)[8]. Although a lot of scientific data has been obtained, there are still many unknown scientific questions to be explored. The Solar Close Observations and Proximity Experiments (SCOPE) program[9,10] aims to observe and detect physical phenomena on the Sun's surface, providing the first ultra-close range in-situ observations of solar activities and solar bursts. It will also obtain coronal magnetic field and plasma parameters in regions with latitudes over 60°. Furthermore, the spacecraft will observe the magnetic reconnection process in solar bursts, with the objective of studying the energy conversion and release mechanisms during this process[11]. A gravity-assist from Jupiter is planned as part of the SCOPE mission, providing an excellent opportunity to expand the scientific objectives of the mission with Jupiter observations[12].

1.2. Intelligent Thermal Control System

In the course of approaching the Sun, the SCOPE spacecraft will accomplish complex orbit transfers and exploration missions. Solar heat flux is only 50 W/m^2 near Jupiter, but it escalates to an extreme of approximately 2.5×10^6 W/m^2 during the approach to the Sun. The spacecraft is accompanied by a wide range of attitude changes close to Jupiter and the solar polar region, resulting in strong changes in the thermal environment. Furthermore, this program has a high requirement for the payload to maintain temperature stability. Consequently, there is an urgent demand for an advanced thermal management system (ATMS) with adaptive control to enable rapid response and prediction of changes in the thermal environment.

At present, Chinese and international research institutions and scholars have been conducting researches on intelligent thermal control strategies for spacecrafts. Yang et al. previously proposed a fuzzy proportion integration shunt-wound control method for the micro-blind mesh, to achieve a high degree of heat density control in a nanosatellite[13]. Liu et al. proposed an Intelligent Agent decision-making architecture applied to the spacecraft thermal control system based on micro-electro-mechanical systems to achieve autonomous thermal control[14]. Guo et al. introduced the development trend of spacecraft thermal autonomous management, including more accurate, more intellectualized and integrate other independently management field[15]. Petkovic et al. proposed a machine learning pipeline for predicting the power of the thermal subsystem on board the Mars Express spacecraft while still maintaining a high prediction performance[16]. Feng et al. proposed a spacecraft intelligent autonomous thermal control method, which uses spacecraft attitude planning to predict the external heat flux in real time to achieve the feedforward control of temperature[17].

1.3. Efficient Liquid Cooling System

According to the characteristics of the mission, the intelligent thermal control process of the ATMS is mainly achieved via fluid cooling. The SCOPE spacecraft is anticipated to encounter significantly varying heat fluxes in orbit, rendering it challenging to maintain suitable temperature ranges for the solar array, platform, and payload modules using conventional heat transfer methods. To facilitate efficient heat collection, transfer, and dissipation, a pumped single-phase liquid cooling loop is proposed as the primary heat transfer technique within the intelligent thermal control system of the SCOPE spacecraft. The China Academy of Space Technology adopted a pumped single-phase cooling loop using perfluorotriethylamine as the working fluid to collect and dissipate heat from the lander-ascender combination[18-20]. The Destiny Laboratory is equipped with a two-stage liquid loop system to control the internal thermal environment[21,22], while the China Space Station core module utilizes a three-stage loop system to collect heat generated within the module and dissipate it into space[23,24]. The Pujiang-1 satellite, developed by the Shanghai Academy of Spaceflight Technology, utilized a micro-pumped liquid loop technique to achieve temperature control and long life cycle requirements[25]. NASA's PSP, which also conducts scientific observations by approaching the Sun, adopts a single-phase pumped water loop as the primary cooling method for its solar array, regulating solar array flap-angle and probe attitude to maintain the temperature of the cooling system within 10−125 °C[26-28]. However, the SCOPE spacecraft will orbit the Sun even closer than the PSP, at an aphelion distance approximately five times farther. The solar irradiance variations the SCOPE spacecraft will be more dramatic, requiring a more complex and challenging design of the solar array cooling system.

1.4. Research Content

Here, we analyze the mission and the thermal environment of SCOPE and propose an ATMS for heat dissipation and temperature stability. This paper is organized as follows: an overview of the mission; thermal environment and ATMS diagram is shown in Section 2; theory and preliminary results of the intelligent thermal control system are given in Section 3; we present design and simulation results for the preliminary liquid cooling system in Section 4; followed by a brief summary. This advanced thermal management research contributes to the development of the SCOPE program and serves as a reference for thermal management in other deep-space exploration initiatives.

2. MISSION ANALYSIS

2.1. Orbital Mission and Thermal Environment Analysis

To accomplish its scientific objectives, the SCOPE program has determined a detection orbit with a perihelion of 5 solar radii ($R_\odot$) from the heliocentricity, aphelion of 125 $R_\odot$, at an inclination of over 60°. The Jupiter gravity-assist (GA) transfer orbit is ultimately selected by comparing the transfer time and fuel consumption. The transfer orbit is depicted in Fig. 1, starting from Earth's escape orbit, performing maneuvers at aphelion, and completing the first deep-space maneuver (DSM). Following the Earth 2:1 gravity-assist, the spacecraft enters the Earth-Jupiter transfer orbit, where the second DSM is carried out during the transit. Scientific observations of Jupiter commence during the flyby. Utilizing the Jupiter gravity-assist, the orbital inclination and perihelion distance are adjusted to achieve an inclination greater than 60° and perihelion of 10 $R_\odot$. In the perihelion phase, electric propulsion is used to decelerate and reduce the orbit period. After 7 cycles of deceleration, the scientific orbit is reached, featuring a perihelion of 5 $R_\odot$ and an aphelion of 125 $R_\odot$. Near the solar perihelion, the solar surface

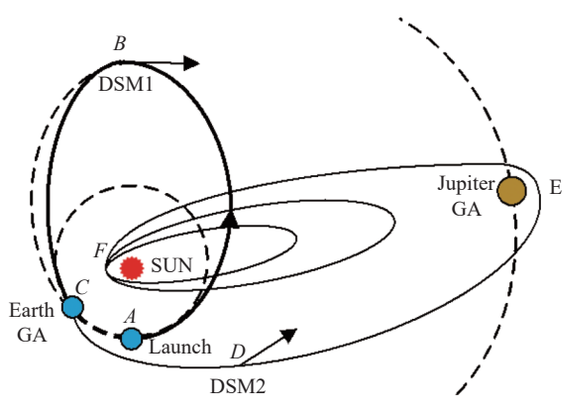

Fig. 1. SCOPE orbital transfer diagram. The spacecraft launches from point *A* to point *B* and performs a DSM. It then reaches point *C* for GA using Earth, changes to an Earth-Jupiter transfer orbit and performs a second DSM at point *D* in the process. A Jupiter-Sun transfer orbit is made through point *E*, using Jupiter for GA. Finally, it reaches the point *F* near the Sun and decelerates several times to achieve the target orbit.

activity in the polar region will be detected and observed.

The use of an Earth-Jupiter gravity-assist for orbital transfer dictates that the spacecraft will encounter a large range of variation in dynamic heat flux. As illustrated in Fig. 2, these variations can be primarily divided into two phases. During the Jupiter flyby, the spacecraft is exposed to a minimum solar heat flux of approximately 50 W/m^2, and after the Jupiter gravity-assist transfer, the spacecraft encounters multiple solar approaches, gradually reducing the aphelion distance, leading to an overall average heat flux increase. The heat flux at perihelion can potentially reach the order of 10^6 W/m^2.

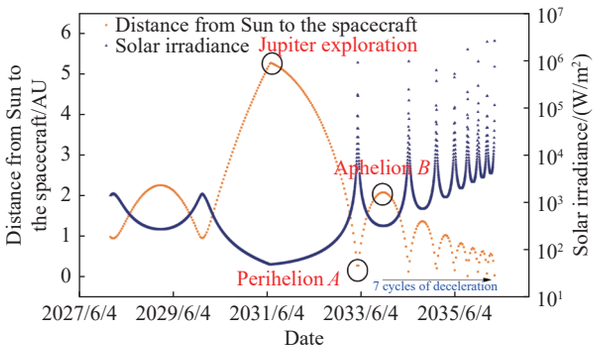

Fig. 2. Environmental heat flux changes during the mission. Yellow dots represent distance from the Sun and blue dots represent solar irradiance. The data in the three circles in the figure represent aphelion of the spacecraft near Jupiter, perihelion, and the aphelion of the spacecraft's first orbit after reaching the Sun.

2.2. ATMS Task Analysis and Composition

The primary function of the ATMS is to integrate components such as the spacecraft payload, platform, solar array, thermal shield, and thermoelectric conversion to achieve optimal heat control and balance between these modules. As illustrated in Fig. 3, the ATMS employs a liquid cooling system and radiation cooling system as heat collection and dissipation carriers, supplemented by the spacecraft's internal heat pipe network. The intelligent analysis and prediction of the thermal environment are conducted using the on-board sensor database and prediction model to facilitate adaptive heat dissipation, heat preservation, and temperature equalization. This method minimizes energy consumption and heat inhomogeneity while meeting the design requirements.

By analyzing the mission characteristics and assigned tasks, the ATMS will primarily concentrate on the exploration of the integrated database, intelligent thermal control system, and efficient liquid cooling system. The architectural framework of the ATMS system is shown in Fig. 4. In addition, to facilitate subsequent research requirements, the ATMS will establish multiple submodule interfaces, integrate new modules into the system through a flexible configuration strategy, and concurrently conduct a global efficiency assessment.

An integrated database, as a vital source of on-board data, serves as the foundation for analysis, prediction, and adaptive control. It incorporates on-board vital databases and a physical model base, which include temperature, orbit parameters, attitude parameters, equipment power consumption, and other relevant data, as well as the information generated by the intelligent thermal control system. The physical model base comprises several submodules such as external heat flux analysis model, network heat transfer analysis model, liquid cooling system analysis model, radiation cooling system analysis model, and node temperature analysis model. During data recording, the

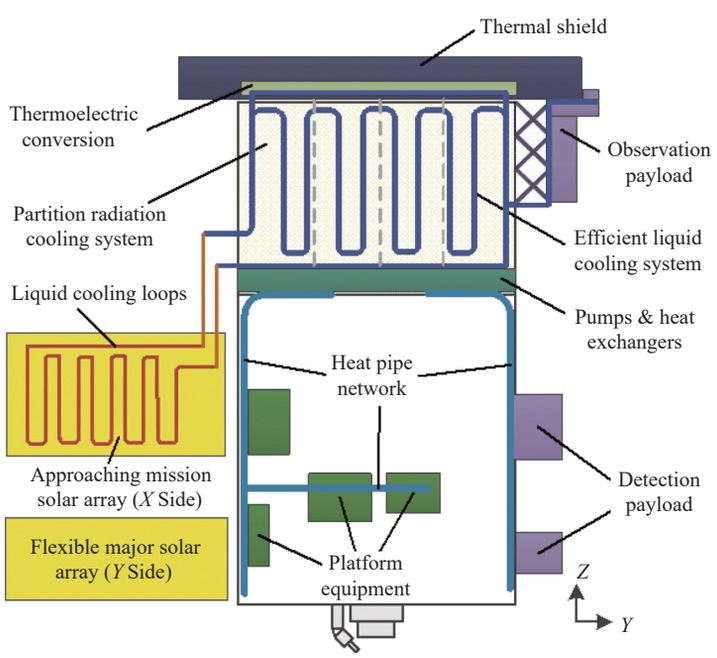

Fig. 3. Schematic diagram showing the ATMS layout. The spacecraft is divided into several parts, such as payload (purple), platform equipment (green), and solar arrays (yellow). By setting up the liquid cooling system and heat exchangers, these parts are distributed for effective thermal control.

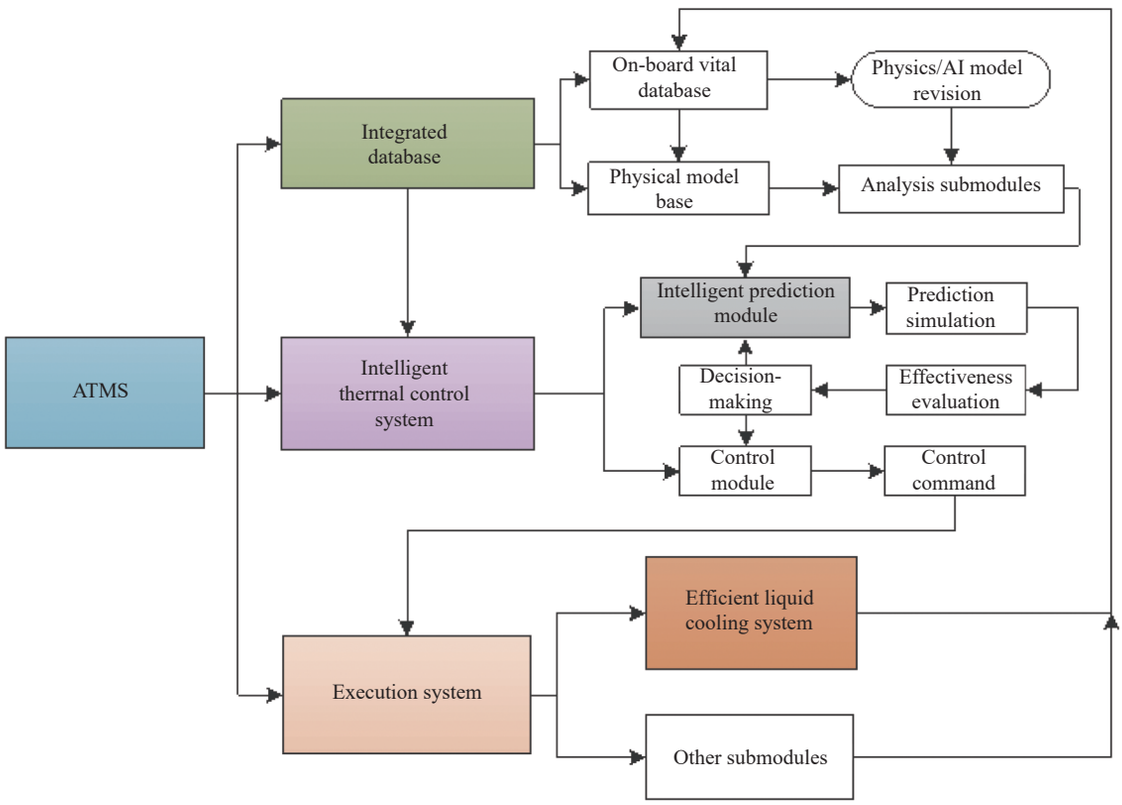

Fig. 4. Architecture of the ATMS.

database updates both data and models through two methods: physical model correction and machine learning correction. The revised information is tagged and stored. As a database that can receive real-time external data and automatically update internal data and models, it plays a crucial role in providing data and model inputs for downstream intelligent thermal control systems.

The intelligent thermal control system is designed to address the challenging temperature control requirements generated by the extreme variation in attitude and orbital distance and solar heating received. This research is centered on three aspects: modular simulation methods for the entire thermal control chain, optimal thermal field planning algorithms based on strategy considerations, and a multidimensional system regulation method. By leveraging thermal environment and heat transfer model predictions, complex thermal field control mechanisms are investigated. Using the heat flux feedforward control method, an adaptive temperature control model is established and a dynamic adaptive thermal control method for multilevel thermal loops is proposed. The quantification and evaluation of temperature sensitivity for a controlled object under varying parameters and high heat flux are presented.

We propose development of high efficiency, low power, and flexible temperature control technology using a pump-driven single-phase liquid loop as a thermal bus. The coupling mechanism between multiple physical fields, such as dynamic flexible fluid-solid heat transfer and medium transport, is investigated. The multilevel design of the coupled heat transfer layout is established between the thermal bus and solar array cooling, payload cooling, radiators, thermal shield, thermoelectric conversion, and platform heat exchangers to achieve effective source heat transport control, residual heat compensation, and waste heat dissipation. In combination with an intelligent thermal control system, the high dynamic management of heat is accomplished through switching between all levels of flow paths within the heat flow bus and flow control, enabling each part to reach its optimal working temperature range.

3. PRELIMINARY RESEARCH AND ANALYSIS OF INTELLIGENT THERMAL CONTROL SYSTEM

3.1. System Introduction

Modular simulation and thermal field planning techniques form the foundation of the intelligent thermal control system for the SCOPE spacecraft. The primary function of modular simulation is to discretize nodes and parameters within the entire thermal chain. This method facilitates the storage of node parameters and module connection parameters in the integrated database, enabling learning and modification of parameters through a vast amount of on-orbit data. The thermal field planning method, which incorporates control theory, monitors the current system state and predicts future conditions to identify the optimal control strategy. Modular simulation accurately simulates the heat exchange relationships between various modules, aiding in the analysis of system performance. Ther-

mal field planning enables real-time temperature adjustments of the spacecraft according to the temperature control requirements of different stages.

3.2. Modular Simulation

Modular simulation involves the decomposition of a complex system into multiple modules, each of which is individually modeled and analyzed. These modules are subsequently docked and simulated, enabling efficient modeling and analysis of intricate systems, as well as multiple physical fields and cross-scale simulation analysis. The specific steps are as follows:

- Model Development: Within the intelligent thermal control system, the spacecraft modules are categorized according to their positions and functions. Each module is treated as an independent subsystem, with corresponding models being established within the modular simulation framework.
- Parameter Assignments: The physical characteristic parameters and control parameters for each module are defined and configured. For instance, the characteristic parameters for equipment encompass temperature, heat capacity, power at varying stages, thermal conductivity and radiation exchange coefficient between equipment and environment.
- System Integration: Using the actual thermal network structure as a basis, each module is interconnected, and the data flow, connections, and control parameters between modules are established to create a comprehensive simulation model for the entire system.
- Simulation and Analysis: The initial parameters are inputted, and optimization conditions are provided. The simulation time and step size are set, allowing the simulation model to run and generate analysis results along with an evaluation of the system's performance at different time intervals.

3.3. Thermal Field Planning

Thermal field planning methods establish appropriate temperature control strategies by assessing target requirements. The planning algorithm adheres to a state-action-cost framework, distinctly defining the state, action, and cost function to pursue globally optimal solutions. The algorithm encompasses stages such as phase division, state delineation, action specification, cost function determination, and policy exploration.

3.3.1. *Algorithm Research*

Employing spacecraft model parameters, we have established the discrete state equation (1) and the goal planning equation (2) for the thermal control system:

$$\begin{aligned}&\boldsymbol{T}(k+1)=\boldsymbol{A}\boldsymbol{T}(k)+\boldsymbol{B}\boldsymbol{u}(k),\\&\boldsymbol{T}(k)=[T_1(k),T_2(k),\cdots,T_n(k)]^{\mathrm{T}},\\&\boldsymbol{u}(k)=\left[u_1(k),u_2(k),\cdots,u_p(k)\right]^{\mathrm{T}};\end{aligned}\tag{1}$$

$$\begin{aligned}&\boldsymbol{T}'(k+1)=\boldsymbol{A}'\boldsymbol{T}'(k),\\&\boldsymbol{T}'(k)=[T_1'(k),T_2'(k),\cdots,T_n'(k)]^{\mathrm{T}}.\end{aligned}\tag{2}$$

In the equations, $\boldsymbol{T}(k)$ represents the state vector, $\boldsymbol{u}(k)$ represents the thermal control vector, and $\boldsymbol{T}'(k)$ represents the system's temperature control objective at step k. The corresponding system state matrix, input matrix, and goal planning matrix are represented by A, B and A', respectively, as follows:

$$\boldsymbol{A}=\begin{bmatrix}a_{11}&\cdots&a_{1n}\\\vdots&\ddots&\vdots\\a_{n1}&\cdots&a_{nn}\end{bmatrix},\ \boldsymbol{B}=\begin{bmatrix}b_{11}&\cdots&b_{1q}\\\vdots&\ddots&\vdots\\b_{n1}&\cdots&b_{nq}\end{bmatrix},$$

$$\boldsymbol{A}'=\begin{bmatrix}a_{11}'&\cdots&a_{1n}'\\\vdots&\ddots&\vdots\\a_{n1}'&\cdots&a_{nn}'\end{bmatrix}.\tag{3}$$

The cost function of the system state from m to x is given by

$$\begin{aligned}J_{m\to x}=&\frac{1}{2}\boldsymbol{e}^{\mathrm{T}}(x)\boldsymbol{R}_1\boldsymbol{e}(x)+\\&\frac{1}{2}\sum_{k=m}^{x-1}\left[\boldsymbol{e}^{\mathrm{T}}(k)\boldsymbol{R}_2\boldsymbol{e}(k)+\boldsymbol{u}^{\mathrm{T}}(k)\boldsymbol{R}_3\boldsymbol{u}(k)\right],\end{aligned}\tag{4}$$

where $\boldsymbol{R}_1$, $\boldsymbol{R}_2$, and $\boldsymbol{R}_3$ represent the system cost weighting matrices. In various flight stages, the thermal control system of the SCOPE mission necessitates the matching of appropriate cost parameters. The physical constraints of system error e and action u are given, respectively, by

$$\boldsymbol{e}(k)=\boldsymbol{T}(k)-\boldsymbol{T}'(k)\tag{5}$$

and

$$\boldsymbol{u}_{\min}(k)\leqslant\boldsymbol{u}(k)\leqslant\boldsymbol{u}_{\max}(k).\tag{6}$$

3.3.2. *Simulation verification*

The coordination of each module can be verified using modular simulation, the correctness of the thermal field algorithm, and control logic. A spacecraft thermal characteristic model is constructed as illustrated in Fig. 5. In an effort to streamline the verification model, a subset of modules within the SCOPE spacecraft is chosen as analysis objects. These modules are analyzed in the form of abstract nodes, with constituent modules including payload, platform, solar array, radiation cooling system, celestial bodies, and space. Among them, the platform temperature T_1, payload temperature T_2, solar array temperature T_3, and radiation cooling temperature T_4 serve as the state variables, given by

$$\begin{cases}\boldsymbol{T}(k)=[T_1(k),\ T_2(k),\ T_3(k),\ T_4(k)]^{\mathrm{T}}\\\boldsymbol{u}(k)=[u_1(k),\ u_2(k),\ u_3(k),\ u_4(k)]^{\mathrm{T}}\end{cases},\tag{7}$$

while u_1, u_2, u_3, and u_4 represent the thermal control power variables for the platform, payload, solar array, and radiators, respectively.

The spacecraft is assigned a set of maneuvers and pay-

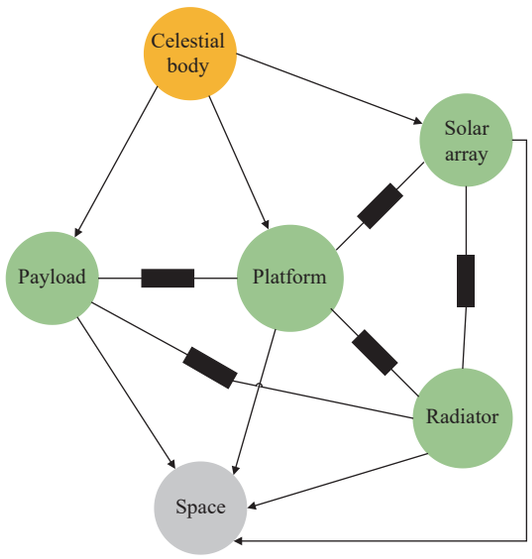

Fig. 5. Spacecraft thermal field characteristic model. Important parts of the spacecraft are established as simulation modules, shown by circles. Black rectangles represent the heat transfer relationship between modules.

load tasks as illustrated in Fig. 6. During payload operations, it is necessary to regulate the temperature of both the payload and platform to the target value, determined by

$$\begin{cases} \boldsymbol{T}'(0) = [5,\ 0,\ 100,\ -20]^{\mathrm{T}} \\ \boldsymbol{T}'(m) = [20,\ 22,\ 100,\ -20]^{\mathrm{T}} \end{cases} \tag{8}$$

while $\boldsymbol{T}'(0)$ represents the spacecraft's temperature field state prior to payload operation, with the characteristic temperatures of the platform, payload, solar array, and radiators being 5 °C, 0 °C, 100 °C, and −20 °C, respectively. $\boldsymbol{T}'(m)$ represents the target temperature at the initiation of payload operations, which are 20 °C, 22 °C, 100 °C, and −20 °C for the platform, payload, solar array, and radiators, respectively.

The thermal field planning can be accomplished by adjusting the parameter values of the weight matrices $\boldsymbol{R}_1$, $\boldsymbol{R}_2$, and $\boldsymbol{R}_3$, as illustrated in Fig. 7. Throughout the entire spacecraft flight process, high control precision is demanded for the platform and payload characteristic temperatures T_1 and T_2, assigned a weight of 1, whereas the precision requirements for the solar array and radiator characteristic temperatures T_3 and T_4 are relatively lower, assigned a weight of 0.1.

Regarding the energy consumption during state transitions, two operational conditions can be identified. In Condition 1, the spacecraft possesses adequate energy, and the anticipated temperature field is expected to achieve the target value in an expedited manner. Consequently, the parameter values of the weight matrix $\boldsymbol{R}_3$ are all set as 0.1. In Condition 2, the spacecraft experiences energy depletion, and the objective is to minimize energy consumption throughout the entire process of reaching the target temperature. Consequently, the parameter values of the weight matrix R_3 are set as 10, 10, 0.1, and 0.1.

The findings reveal that under Condition 1, the platform and payload temperatures can attain the target levels comparatively swift, albeit at a higher energy cost. Under Condition 2, the temperature control objective can be reached with reduced energy consumption, albeit requiring a longer duration. The simulation process can verify the coordination of each module and the correctness of the algorithm and control. This study shows that by establishing weight parameters and integrating intelligent analysis methods, the cost of achieving the objectives can be strategically planned.

4. EFFICIENT LIQUID COOLING SYSTEM

4.1. System Principle and Preliminary Design

The solar arrays are significant for the energy supply

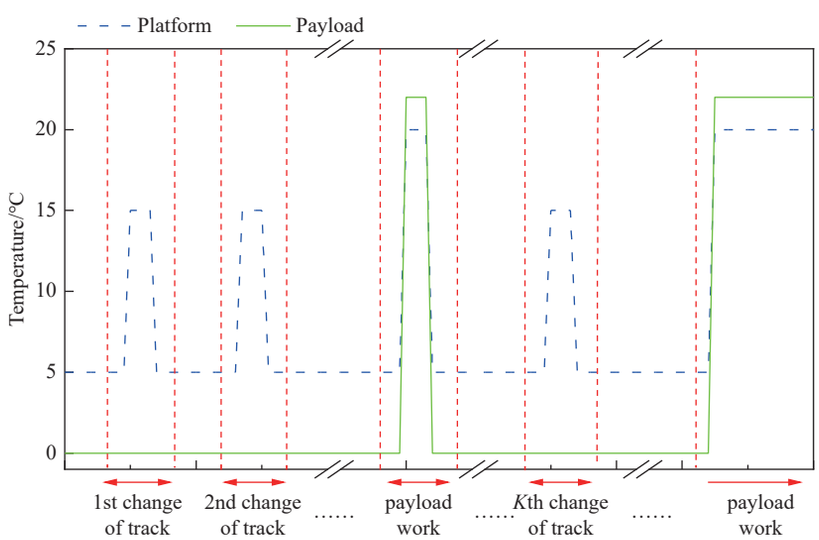

Fig. 6. Mission planning for simulation analysis. The blue dotted line and green solid line represent the temperature control targets of the platform and payload equipment respectively, and the red arrows represent different working stages.

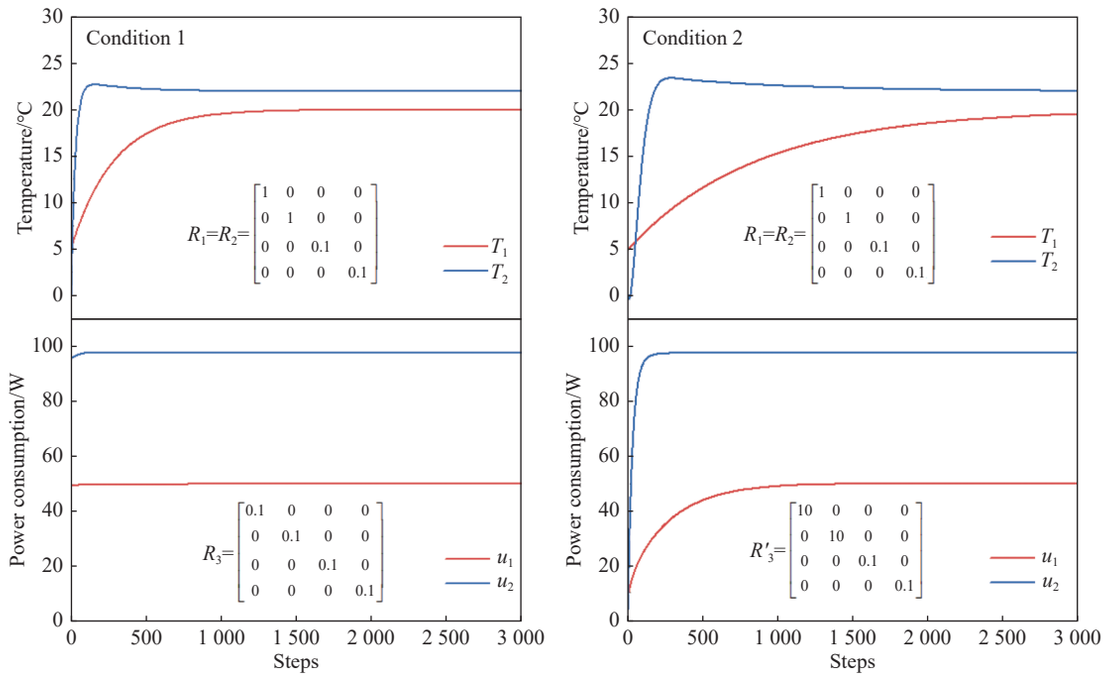

Fig. 7. Temperature regulation results under different conditions.

of the SCOPE spacecraft. Because of the extremely complex thermal environment, research on the cooling technique for solar arrays is given priority. The design of the solar arrays must meet the minimum energy demand under the most severe solar irradiance conditions during the spacecraft flyby of Jupiter, and consider the temperature control when the spacecraft approaches the Sun:

(1) Considering that the energy demand for stand by operation is 200 W and the solar irradiance will decrease to 50 W/m^2 as the spacecraft approaches Jupiter, the area of the solar array needs to be 28 m^2.

(2) The maximum solar distance at aphelion of the solar scientific orbit is about 2.08 AU. Given that the energy demand for science operation is 300 W, the required area of solar array is approximately 10 m^2.

(3) At the perihelion of the solar scientific orbit, the ratio of heat to electricity is as high as 50:1. The effective area of the solar arrays normal to the Sun is approximately 0.01 m^2.

An efficient liquid cooling system is designed to control the temperature of the two solar arrays at the solar close-up observation stage. The requirements of the advanced liquid cooling system are as follows:

- The solar array temperature is required within a range from −150 °C to 150 °C.
- The radiator temperature is required to be higher than −30 °C after the system is filled with working fluid.
- The system is required to have a heat dissipation capacity of no less than 7500 W for a single solar array due to the ratio of heat to electricity being 50:1.
- The temperature range of the working fluid in the system is from −20 °C to 160 °C.

An advanced pumped liquid cooling system is designed, as shown in Fig. 8, containing two cooling plates, four radiators, two pumps, an accumulator, valves, and pipelines. As shown in Fig. 2, at the solar scientific orbit, the distance between the spacecraft and the Sun varies widely (0.023−2.08 AU), resulting in a four-order-of-magnitude variation in solar irradiance. Therefore, to avoid freezing or vaporization of the fluid under extreme conditions, a working fluid needs to be selected for the cooling system with a low triple point and high boiling point (relatively low saturated vapor pressure). For this purpose, a 50% ethylene glycol aqueous solution is selected, and its key thermal properties are shown in Table 1.

According to the SCOPE mission and orbit design, there are several important events for the solar array liquid cooling system during the spacecraft flight, as follows:

(1) During the launch phase, orbit transfer phase, and Jupiter exploration phase, the working fluid is stored in the accumulator, and the temperature is actively controlled to be maintained at above −10 °C. At the same time, the radiator surface of the advanced pumped liquid cooling system is kept closed to reduce external radiation, and thermal compensation is provided to keep the temperature higher than −150 °C.

(2) When the spacecraft reaches approximately 1 AU from the Sun, after flying by Jupiter, the radiators of the cooling system are opened, and the attitude is adjusted so that the radiators face the Sun. The ATMS will monitor the radiator temperature in real time and open the control valve at the accumulator outlet to allow liquid into the loop when the temperature is not lower than 0 °C.

(3) During approach to the Sun, based on the external heat flux, energy demand, and temperatures of the solar arrays, the ATMS outputs signal for the rotation mechanism to gradually tilt the solar panels to the shadow

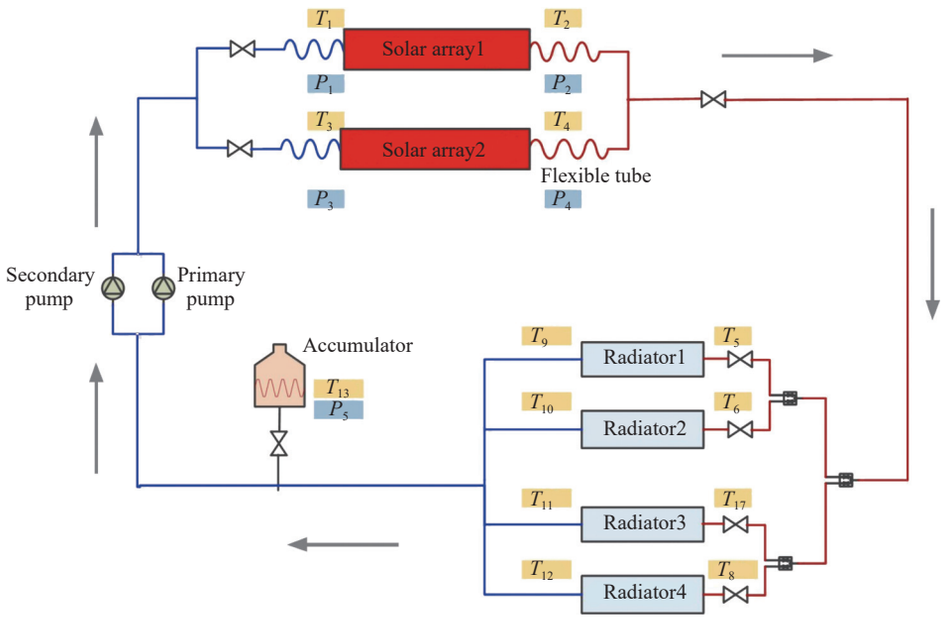

Fig. 8. Pumped liquid cooling system composition. The fluid flows in the direction of the grey arrows, absorbs heat from the solar arrays and then releases heat to the radiators.

Table 1. Thermal properties of 50% ethylene glycol aqueous solution

Properties	Value
Triple point (K)	239.4
Saturated vapor pressure at 200 °C (MPa)	1.2
Thermal conductivity (W/m·K)	0.39
Specific heat (J/kg/K)	3285.4
Viscosity (mPa·s)	0.37

under the thermal shield to reduce heat input.

(4) After the first close-up observation, the spacecraft will fly from the perihelion (0.023 AU) to the aphelion (2.08 AU). The angle of the solar panels will be increased to ensure the stability of the energy supply. To ensure the lowest temperature of the liquid in the loop, it is considered to close two radiators and adjust the attitude to make another two radiators face the Sun.

4.2. Analysis of the Cooling System under Different Working Conditions

A simulation model is created for the advanced liquid cooling system, as shown in Fig. 9. The main components of the system include two cooling plates for the solar arrays with an area of 5 m^2 each, four radiators with an area of 2.5 m^2 each, an accumulator, a liquid source, valves, and pipelines. The flow rate is 0.1 kg/s, and the system operating pressure is not less than 0.5 MPa.

4.2.1. *Simulation Results for High-Temperature Conditions at Perihelion*

The spacecraft will achieve perihelia as close as 0.023 AU from the Sun. The heat flux input of a single solar array at perihelion is estimated to be 7 500 W. The initial temperature of the cooling system is 20 °C, and the steady-state simulation results are shown in Fig. 10. The maximum temperature of the solar array is 90.6 °C, the maximum outlet temperature of the cooling plate is 88.9 °C, and the maximum inlet temperature of the cooling plate is 68.9 °C, which meet the design requirements.

4.2.2. *Simulation Results for Low-Temperature Conditions at Aphelion*

After a close exploration of the Sun, the spacecraft will fly toward aphelion at 2.08 AU. During this process, the solar panel will be deployed at 0.8 AU to ensure a sufficient energy supply. To investigate the heat transfer performance of a solar array cooling system during the transition from high-temperature to low-temperature states, a system dynamic simulation is conducted. When the solar distance increases to 1.05 AU, the spacecraft attitude is adjusted to make radiators 1 and 2 face the Sun, while radiators 3 and 4 remain closed. After the spacecraft passes aphelion, the distance to the Sun decreases again to 1.05 AU, and the spacecraft attitude is adjusted to make the thermal shield face the Sun as radiators 3 and 4 are opened. The simulation results are shown in Fig. 11, at time t_1. Due to the influence of the attitude adjustment and the closing of the radiators, the temperature of the solar array cooling system increases. Subsequently, as the solar distance gradually increases and solar irradiance decreases, the temperature of the cooling system decreases, reaching a minimum temperature of −12.8 °C at aphelion. The results show that the system meets the design requirement of the working fluid temperature of ≥ −20 °C during operation.

As mentioned above, the simulation results show that the temperature of the solar array at perihelion (~0.023 AU) is 90.6 °C, and the minimum fluid temperature at aphelion (~2.08 AU) is −12.8 °C, meeting the sys-

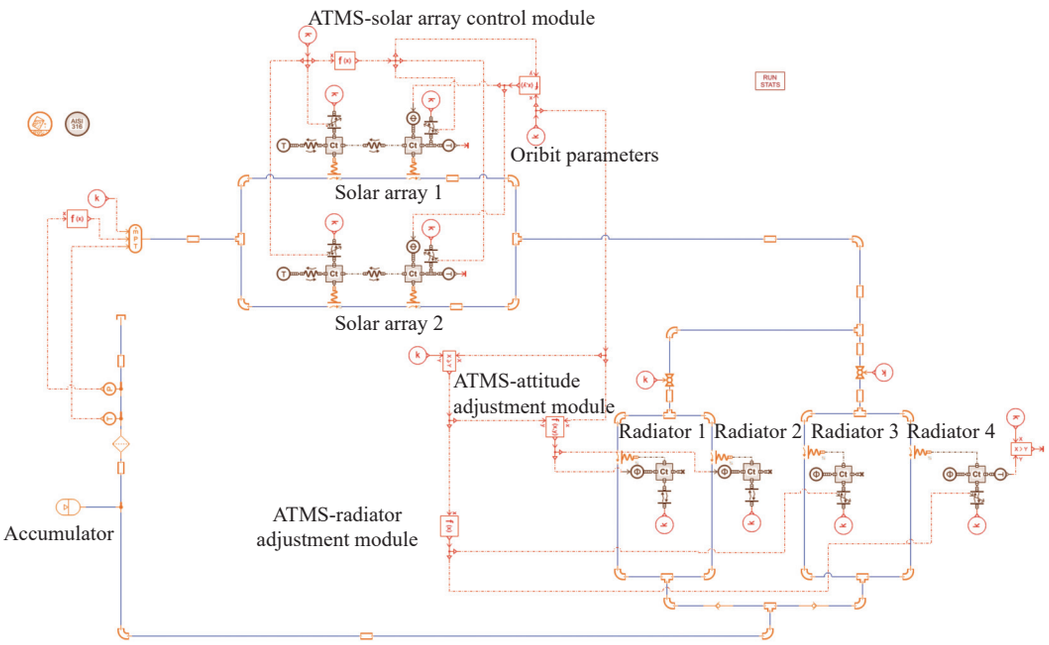

Fig. 9. Solar array simulation model for the advanced pumped liquid cooling system, consisting of of flow source, solar arrays, radiators, accumulator, pipes, and several control modules, which are used to adjust the folding angle of solar arrays, the attitude of the spacecraft, and the heat dissipation area of radiators.

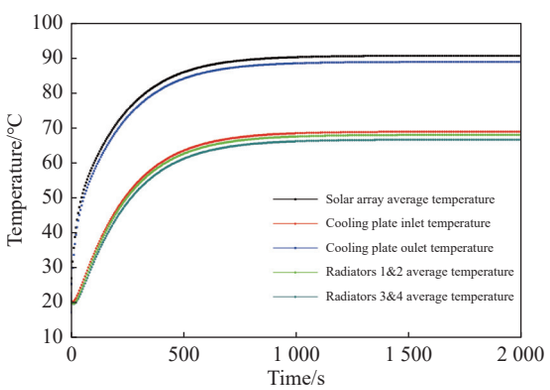

Fig. 10. Simulation results at perihelion.

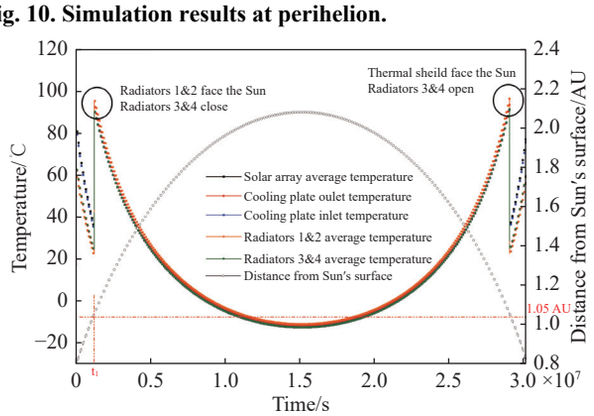

Fig. 11. Simulation results at aphelion.

tem design requirements.

5. CONCLUSION

In this paper, a comprehensive analysis is presented for SCOPE, focusing on the orbital transfer mission and the characteristics of the thermal environments. The study proposes the necessary functions and desired effects to be achieved in an ATMS. The core of this system revolves around an integrated database, intelligent thermal control methods, and efficient fluid loops, with careful consideration given to system architecture relationships and layout design. The proposed modular simulation method for spacecraft achieves the simulation of the entire thermal control system by modeling and integrating each module. Through case verification, the thermal field planning algorithm successfully accomplishes optimal regulation of the spacecraft's thermal field. The design and implementation of the solar array cooling system have been conducted, including the establishment of a comprehensive system model and dynamic simulation under extreme working conditions at perihelion and aphelion during solar detection. The simulation results demonstrate that the cooling system successfully fulfills the design requirements in this stage.

In subsequent studies, it is imperative to update the design in a timely manner, in accordance with scientific missions and technical requirements. Consequently, it is necessary to condense and assign key technical indices of ATMS. Furthermore, research will be conducted on global sensing, intelligent decision-making, and real-time execution. Additional advancements are required for system components such as the deployment mechanism for the radiation cooling system, and a flexible fluid pipe. Research on an advanced thermal management system for SCOPE will contribute to the development of the SCOPE program and serves as a reference for thermal management in future deep-space exploration missions.

ACKNOWLEDGEMENTS

This study is supported by National Key R&D Program of China (2022YFF0503800).

AUTHOR CONTRIBUTIONS

Liu Liu conceived the idea, prepared data curation, provided investigation support, wrote original draft and edited the manuscript. Kangli Bao and Jianchao Feng prepared data curation, provided investigation support, used software for simulation analysis and wrote original draft. Xiaofei Zhu and Haoyu Wang provided investigation support, used software for simulation analysis and wrote original draft. Xiaofeng Zhang played the project administration and supervision role. Jun Lin supported the funding acquisition. All authors read and approved the final manuscript.

DECLARATION OF INTERESTS

Xiaofeng Zhang is editorial board member and Jun Lin is the executive editor-in-chief for Astronomical Techniques and Instruments, they were not involved in the editorial review or the decision to publish this article. The authors declare no competing interests.

REFERENCES

[1] Lemen, J. R., Title, A. M., Akin, D. J., et al. 2012. The atmospheric imaging assembly (AIA) on the solar dynamics observatory (SDO). *Solar Physics*, **275**(1-2): 17−40.

[2] Pesnell, W. D., Thompson, B. J., Chamberlin, P. C. 2012. The solar dynamics observatory (SDO). *Solar Physics*, **275**(1-2): 3−15.

[3] Bale, S. D, Badman, S. T., Bonnell, J. W., et al. 2019. Highly structured slow solar wind emerging from an equatorial coronal hole. *Nature*, **576**: 237−242.

[4] Müller, D., Cyr, O. C. St., Zouganelis, I., et al . 2020. The solar orbiter mission. *Astronomy & Astrophysics*, **642**: A1.

[5] Gan, W. Q., Zhu, C., Deng, Y. Y., et al. 2019. Advanced space-based solar observatory (ASO-S): an overview. *Research in Astronomy and Astrophysics*, **19**(11): 5−12.

[6] Li, H., Che, B., Feng, L., et al. 2019. The Lyman-alpha solar telescope (LST) for the ASO-S mission — I scientific objectives and overview. *Research in Astronomy and Astrophysics*, **19**(11): 25−34.

[7] Deng, Y. Y., Zhang, H. Y., Yang, J. F., et al. 2019. Design of the full-disk magnetoGraph (FMG) onboard the ASO-S. *Research in Astronomy and Astrophysics*, **19**(11): 11−22.

[8] Li, C., Fang, C., Li, Z., et al. 2022. The Chinese Hα Solar Explorer (CHASE) mission: an overview. *SCIENCE CHINA Physics, Mechanics & Astronomy*, **65**(8): 2−9.

[9] Lin, J., Wang, M., Tian, H., et al. 2019. In situ measurements of the solar eruption. *SCIENTIA SINICA Physica, Mechanica & Astronomica*, **49**(5): 70−89. (in Chinese)

[10] Lin, J., Huang, S. J., Li, Y.,et al. 2021. In situ detection of the solar eruption: lay a finger on the Sun. *Chinese Journal of Space Science*, **41**(2): 183−210. (in Chinese)

[11] Lin, J. 2019. Lin-Forbes model of solar eruptions and turbulent properties of large-scale magnetic reconnection. http://www.pmo.cas.cn/cxwh/colloquium/202112/t20211203_6287097.html.

[12] Yao, Z. H., Sun, T. R. 2022. Origin of Jupiter's soft X-ray aurora and a brief perspective on future explorations. *Reviews of Geophysics and Planetary Physics*, **53**(2): 236−237. (in Chinese)

[13] Yang, J., Li, Y. Z., Wang, J. 2008. Research and simulation on thermal control technology of Nanosatellite micro-shutters. *Strategic Study of CAE*, **10**(7): 169−172. (in Chinese)

[14] Liu, J., Li, Y. Z., Zhang, J. X. , et al. 2009. Research on MEMS autonomous thermal control system of spacecraft based on intelligent Agent. *Spacecraft Environment Engineering*, **26**(6): 574−579. (in Chinese)

[15] Guo, J., Chen, Y., Shao, X. G. 2012. Intelligent control technology for spacecraft thermal autonomous management. *Spacecraft Engineering*, **21**(06): 49−53. (in Chinese)

[16] Petkovic, M. , Boumghar, R., Breskvar, M., et al. 2019. Machine learning for predicting thermal power consumption of the Mars express spacecraft. *IEEE Aerospace and Electronic Systems Magazine*, **34**(7): 46−60.

[17] Feng, J., Zhang, X., Liao, X., et al. 2021. Spacecraft intelligent autonomous thermal control method based on space environment prediction. *Spacecraft Engineering*, **30**(5): 45−52. (in Chinese)

[18] Ning, X. W., Xu, K., Wang, Y. Y., et al. 2022. Design and implementation of Chang'e-5 complex of lander and ascent vehicle lightweight pumped fluid loop thermal bus. *Acta Aeronautica et Astronautica Sinica*, **43**(12): 164−173. (in Chinese)

[19] Xiang, Y. C., Liu, Z. J., Ning, X. W., et al. 2022. Review of thermal control technology in Chinese lunar probes. *Spacecraft Engineering*, **31**(2): 29−34. (in Chinese)

[20] Wang, Y. Y., Ning, X. W., Miao, J. Y., et al. 2021. Work performance analysis on the Chang'e-5 lunar lander water sublimation heat dissipation system. *Scientia Sinica(Technologica)*, **51**(12): 1445−1452.

[21] Chen, Z. F., Xu, Y. D., Guo, T., et al. 2013. Internal active thermal control system of international space station. *Aerospace Shanghai*, **30**(3): 27−32. (in Chinese)

[22] Patel, V. P., Winton, D., Ibarra, T. H. 2004. A selected operational history of the internal thermal control system (ITCS) for international space station (ISS). *SAE Technical Paper*, 2004-01-2470.

[23] Ning, X. W., Li, J. D., Wang, Y. Y., et al. 2019. Review on construction of new spacecraft thermal control system in China. *Acta Aeronautica et Astronautica Sinica*, **40**(7): 6−18. (in Chinese)

[24] Fu, S. M., Xu, X. P., Pei, Y. F. 2010. Modeling and analysis of space station integrated global thermal mathematical models. *Spacecraft Environment Engineering*, **27**(1): 75−79. (in Chinese)

[25] Cao, J. G., Gu, Y. P., Chen, G., et al. 2017. The flight experiments of active thermal control system with micro-mechanical pumped fluid loop. *Spacecraft Environment Engineering*, **34**(4): 343−349. (in Chinese)

[26] Lockwood, M. K. , Ercol, C. J., Cho, W. , et al. 2010. An active cooling system for the solar probe power system. In Proceedings of 40th International Conference on Environmental Systems.

[27] Ercol, C. J., Abel, E. D., Allan, H. G., et al. 2018. Thermal design verification testing of the solar array cooling system for parker solar probe. In Proceedings of 48th International Conference on Environmental Systems.

[28] Congdon, E. A. 2021. Multi-scale thermal and structural characterization of carbon foam for the parker solar probe thermal protect system. Doctor thesis, Johns Hopkins University.